Optimization of a Robot for Handling Glass Plates

Nicolò D'Alfio, Gabriella Eula*

Department of Mechanics, Politecnico of Turin Technical University
C.so Duca degli Abruzzi 24, 10129 Torino, Italy
*Phone: + 39-11-5646911; E-mail: gabriella.eula.@polito.it

***Abstract**: The paper discusses the optimization of a structure connected to a set of pneumatic holdfasts. This equipment is mounted on an articulated robot arm with 6 degrees of freedom and is used to handle float-glass plates on a production line.*
The robot transfers float-glass plates from a horizontal to a vertical position, rotating them 90° around the robot's principal axis.
The structure's actual geometry was analyzed and redesigned to reduce weight, investigating stress and strain on the old and new systems using an FEM code in both static and dynamic operating conditions.
Results are presented in diagrams showing bending moment, shear stress and structure strain-stress whereby a new lightweight geometry can be selected which reduces inertial forces during robot operation.
Results are highly satisfactory and show excellent potential for improving robot performance and geometry.

***Keywords**: review of industrial robot applications; new designs and prototypes; reengineering in robotics; construction robots; automation*

I INTRODUCTION

In the glass industry, product handling is one of the major challenges for designers of production systems. The following investigation analyzes a frame connected to a robot used to handle float-glass plates by means of suction cup-type pneumatic holdfasts. This analysis is conducted using an FEM computing code [1]-[5].
The robot is a commercial unit whose end effector consists of a frame carrying a set of pneumatic holdfasts which grip the glass. The robot is illustrated in Figure 1. It features six degrees of freedom, ±180° arm rotation, 2750 kg mass and 500 kg payload. The frame and holdfasts are also shown.

a)

b)

Figure 1
a) Robot with frame installed, b) Holdfast frame

Frame geometry is depicted in the drawings below (Figure 2). As the center of the wrist does not correspond to the glass plate's center of gravity, not all of the holdfasts are uniformly stressed.

Figure 2 shows the aluminum sections used as the system's load-bearing elements, the pneumatic holdfasts, a set of sensors whereby the presence of the glass plate can be detected, and several spacer units. As can be seen, the holdfasts feature a bellows configuration to compensate for any frame distortion.

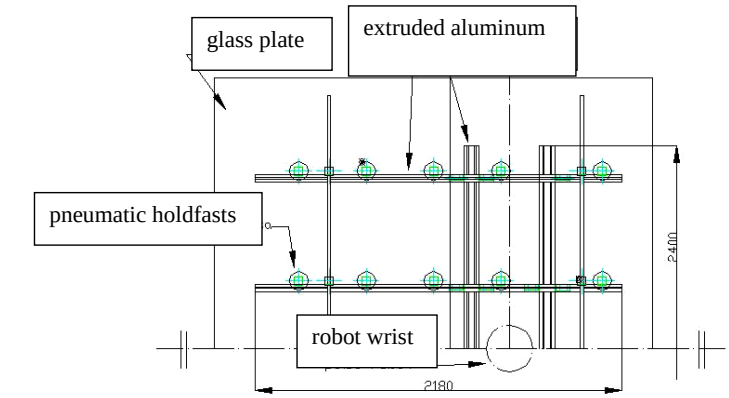

a)

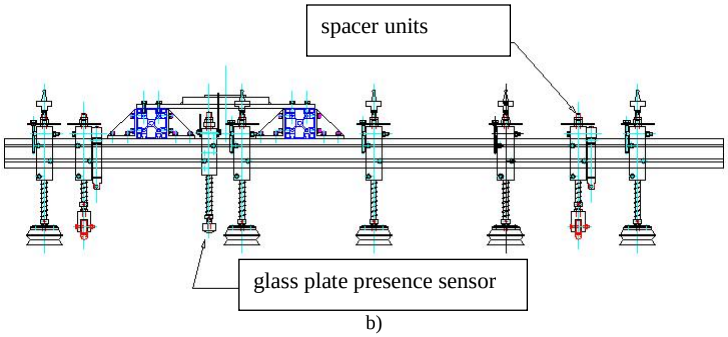

b)

Figure 2
a) Top view of frame; b) Side view of frame

The extruded aluminum sections used for the frame have the following mechanical properties: area = 2270 mm^2; inertias I_{XX}=1740010.27 mm^4, I_{YY}=1740010.27 mm^4, I_{ZZ}=3480020.55 mm^4, I_{polar}=3480020.55 mm^4, $I_X=I_Y$=1740010.27 mm^4; material Al Mg Si 0.5 F25; linear density 6.20 kg/m; section dimensions 90 x 90 mm. Two extrusions of this type with a length of 2400 mm are used. They support a further four sections connected to the robot wrist by means of a perforated plate whose properties are: area=1165 mm^2; inertias I_{XX}=930195.13 mm^4, I_{YY}=240327.47 mm^4, I_{ZZ}=1170522.59 mm^4, I_{polar}=1170522.59 mm^4, I_X= 240327.47 mm^4 I_Y=930195.13 mm^4; material Al Mg Si 0.5 F25; linear density 3.310 kg/m; section dimensions 45 x 90 mm.

II DEVELOPMENT OF THE FRAME MODEL

In the case in question, it is clear that the frame has an axis of symmetry (Figure 2). Consequently, it is sufficient to model one half of the structure with an FEM code, applying an appropriate constraint that simulates the presence of the other half of the system.

The nodes are located at each point of connection between the aluminum sections and at each holdfast unit so that loads can be applied. The origin of the coordinates corresponds to the center of the robot wrist (Figure 3a).

Figure 3a shows the nodes at the points with the holdfast units, while nodes 2 and 7 are located at the positions where the plate attached to the robot wrist is connected to the frame.

It should be noted that the element chosen for simulation also permits the end nodes to be connected away from the center of the beam, or in other words to make connections (see node 8) between the 45x90 mm sections and the 90x90 mm sections.

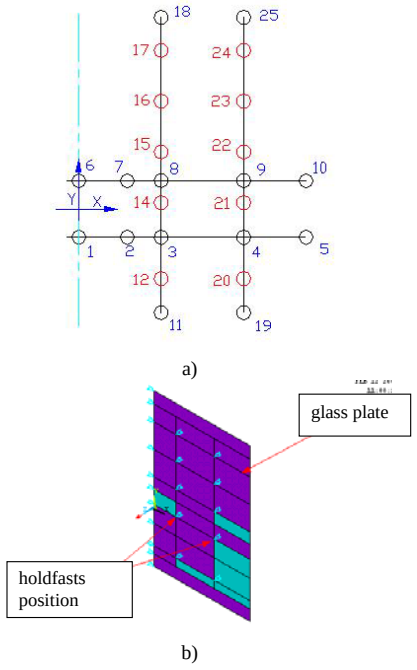

Figure 3
Location of nodes

The selected element is characterized by a local reference system (x,y,z), with the x axis corresponding to the longitudinal axis of the beam (passing through the section's center of gravity), while the y axis is oriented so that it is parallel to the X-Y plane of the global reference system (X,Y,Z). The input data that must be provided include the elastic modulus and Poisson's ratio of the material used. For aluminum, these values are as follows: modulus of elasticity E = 70000 MPa; Poisson's ratio $\nu = 0.3$. A schematic view of the frame

constructed for finite element analysis is shown in Figure 3b.

III ASSESSING STATIC AND DYNAMIC STRESSES

The static stresses on the frame when the glass plate is suspended from the holdfasts in the horizontal position (A) were assessed first (Figure 4).

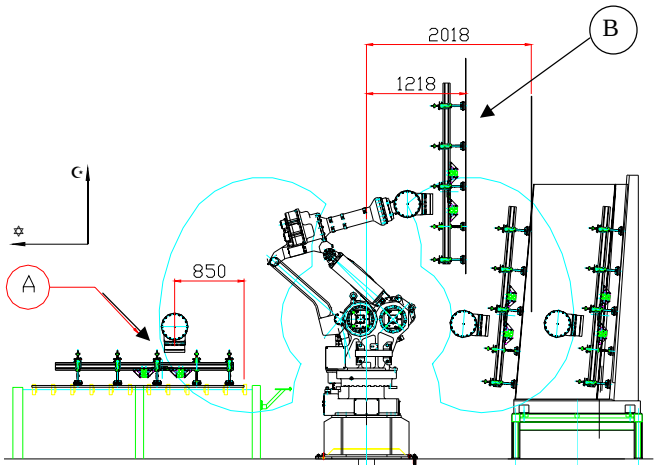

Figure 4
Glass unloading zone

In the model, the frame was constrained at the points of connection between the structure and the plate which is positively connected to the robot wrist: thus, all rotation and translation on the part of nodes 2 and 7 was prevented.

In addition, as it was necessary to simulate the condition of symmetry, nodes 1 and 6 cannot move along the X axis.

Applied loads are due to the weight force of the holdfast units, the aluminum sections and the carried glass (Figure 5).

Consequently, P_T also includes the weights of the holdfast units (P_V).

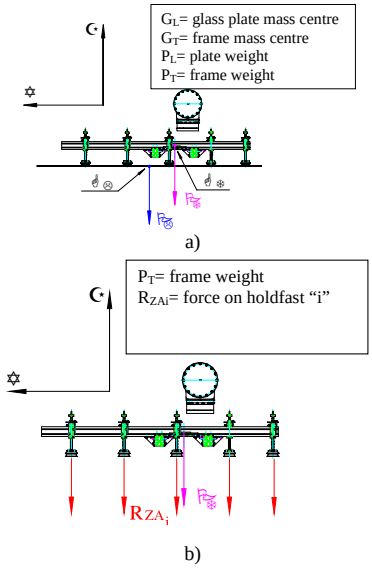

Figure 5
Forces diagram of the glass + frame system

The weight force on the holdfast units was simulated using the model shown in Figure 5, where the gravitational field is unloaded uniformly on each node, at which constraint reaction force R_{Zai} is located.

Figure 6 shows the distribution of these reactions, which vary from 6 to 184 N, on the holdfasts.

The center of gravity of the glass plate is 450 mm in direction +Y from the center of the robot wrist.

In this way, the holdfasts located farther from the robot wrist receive a larger fraction of the weight of the glass plate because of the latter's overhang.

The value of R_{ZA} at node 16, moreover, is positive rather than negative like the others, because of the relative position of the applied load and nodes 16 and 17.

As can be seen from the following free body diagrams, the reaction forces R_{ZA} thus obtained, added to the contribution due to the weight P_V of the holdfast units, will stress the frame with a force $F_{ZA} = P_V + R_{ZA}$ (Figure 8) acting on the structure and varying from 14 to 200 N.

The first item to be analyzed is the frame's strain state, and in particular its displacement along the Z axis as shown in Figure 7.

In this connection, it should be noted that stress analysis is linked to the equilibrium of the global system by the following expression:

$$\int_S \{r\} \wedge \{p\} dS + \int_\Omega \{r\} \wedge \{t\} d\Omega + \int_V \{r\} \wedge \{F\} dV = 0 \qquad (1)$$

where: $\{r\}$ = body point position vector; $\{p\}$ = distributed force vector per unit surface; dS = infinitesimal body frontier surface; $\{t\}$ = stress vector; dΩ = infinitesimal area; $\{F\}$ = force vector per unit volume; dV = infinitesimal volume.

It is important to determine whether preferential directions where only normal stresses are present arise in body, on the basis of which we have

$$\{t_n\} = \sigma_n \{n\} \qquad (2)$$

where $\{t_n\}$ = normal stress vector; σ_n = normal stress; $\{n\}$ = normal vector.

Strains are then calculated using the differential equation of the elastic line, expressed as:

$$\frac{d^2 v}{dZ^2} = -\frac{M_x}{EI_x} \qquad (3)$$

where v = vertical displacement (along the Z axis); Z = beam axis; M_x = bending moment around the x axis; E = elastic modulo; I_x = moment of inertia relative to X [6].

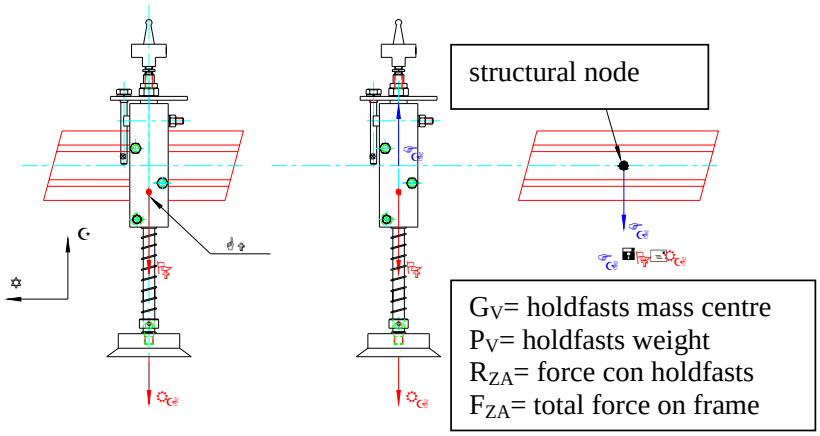

Figure 6
Forces acting on a generic frame node

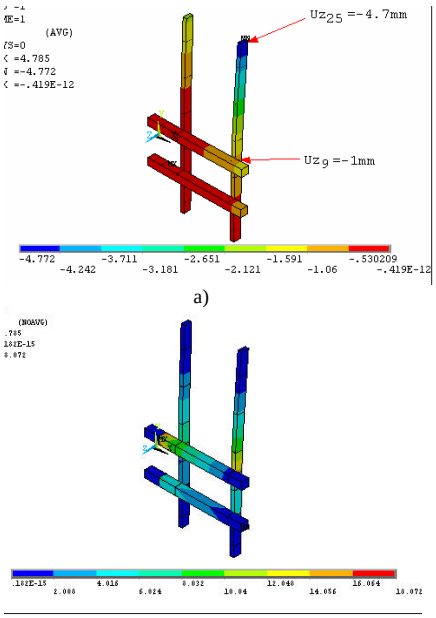

a)

b)

Figure 7
a) Strain state; b) Stress state

As can be seen from Figure 7, the frame is clearly not optimized: three of the four beams are highly stressed, and the structure as a whole is extremely bulky.

This means that Uz is between 0 and -0.53 mm. As a maximum displacement of 4.77 mm occurred at node 25, the effective deflection is 3.77 mm.

The stresses to which the structure is subjected can be analyzed by plotting the internal stress characteristics.

The shear curve can be interpolated to assess its range of variation, which is ±450 N. The bending moment, on the other hand, ranges from –0.290 to 88.784 Nm.

The Von Mises criterion was applied in order to obtain an equivalent stress value (Figure 7b).

The stresses thus determined must be taken as an indicator of the stresses due to bending alone, without considering the complexity of the beams' cross-sectional geometry and the resulting notch effects, etc.

Taking the latter into account would call for a further simulation centering only on the cross section.

The preceding simulations considered the static stresses acting on the frame.

We will now analyze the stresses arising from the inertia forces occurring when the glass plate is moved (dynamic conditions). Calculations focus on the centrifugal forces. To investigate these forces, a precise geometrical configuration must be established for the robot. As can be seen from the drawing of the unloading zone, the most critical condition is that designated by the letter B (Figure 4), where the glass plate is in the vertical position and robot motion consists only of a rotation by joint 1. The maximum distance between the glass plate and the axis of rotation is 2 m (Figure 8). In this case, the centrifugal forces can be quantified, as centripetal acceleration is known to be 2.9 m/s^2. These forces are due to three factors: the mass of the holdfast units, the mass of the aluminum sections, and the mass of the glass plate. Total centrifugal force is thus approximately 500 N. The values of the constraint reaction along the Z axis represent the forces that are unloaded on the holdfasts as a result of dynamic stresses. The same technique employed earlier can also be used to assess the forces that the holdfasts must exert on the glass in order to balance the weight force, which in configuration B (Figure 4) acts in direction -Y. The constraint reactions on the holdfasts due to centrifugal force and the weight force vary between 1 and 50 N along the Z axis and between 50 and 90 N along Y. An analysis of these values shows certain analogies with the static case: maximum values of R_{ZB} always occur at the holdfasts located farthest from the robot wrist because of the fact that the centrifugal force and the weight force depend on centripetal and gravitational acceleration respectively. In addition, they are linked to the distribution of the system's total mass resulting from the nodes selected for the structure. Thus, the corresponding constraints will also be similarly distributed. As can be seen, the values for forces R_{ZB} now differ from those for the static case in that they are all of the same sign: this is due to the fact that centripetal acceleration (2.9 m/s^2) is less than gravitational acceleration, and the constraint reaction thus no longer changes sign on node 16. The total reactions unloaded on the load-bearing structure can be determined by analyzing the free body diagrams for a holdfast unit (Figure 9). By contrast with the static case, when the glass plate is maintained in the vertical position, bending moments now arise which are concentrated on the holdfast units. These stresses are equal to:

$$M(O) = R_{YB} \cdot B + P_V \cdot A \cong R_{YB} \cdot B \qquad (4)$$

as the holdfast unit's weight moment $(P_V \cdot A)$ is negligible by comparison with that of the reactions R_{YB}.

The stresses acing on the carrier frame will thus be between 70 and 120 N along Y, between 7 and 70 N along Z, and between 12350 and 27932 Nmm around X. Strains on the frame under dynamic conditions are illustrated in Figure 9 a and b.

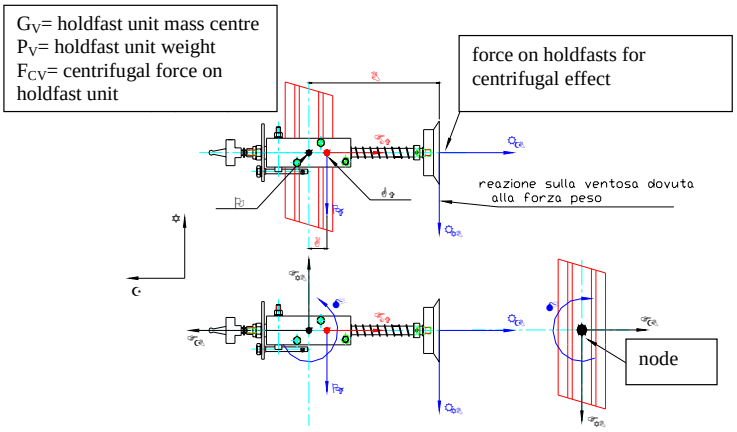

Figure 8
Forces acting on a holdfast unit

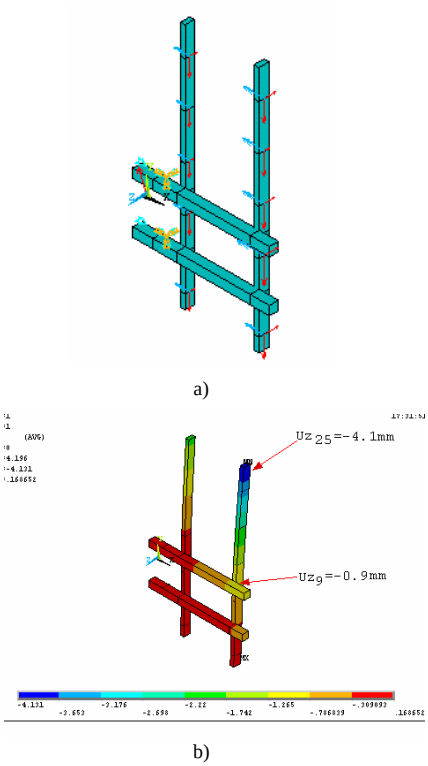

Figure 9
a) Static and dynamic forces b) Frame deflection

IV FRAME OPTIMIZATION

To optimize the system, a number of different aluminum sections which could replace those currently used for the frame were analyzed, attempting to reduce the structure's weight. Properties of several of the components taken into consideration were as follows: area=1486 mm^2; inertias I_{XX}=1006900.13 mm^4, I_{YY}=240327.47 mm^4, I_{ZZ}=1006900.13 mm^4, I_{polar}=2013800.16 mm^4, $I_X=I_Y$=1006900.13 mm^4; material Al 6061; linear density 4.01 kg/m; section dimensions 80 x 80 mm. Sections with the following properties were chosen to replace the two main beams: area=890.2 mm^2; inertias I_{XX}=578100 mm^4, I_{YY}=151500.47 mm^4, I_{ZZ}=729600,47 mm^4, I_{polar}=729600.47 mm^4, I_X= 151500.47 mm^4 I_Y=578100.00 mm^4; material Al 6061; linear density 2.42 kg/m; section dimensions 40 x 80 mm.

Strain plots for the optimized frame are shown in Figure 10.

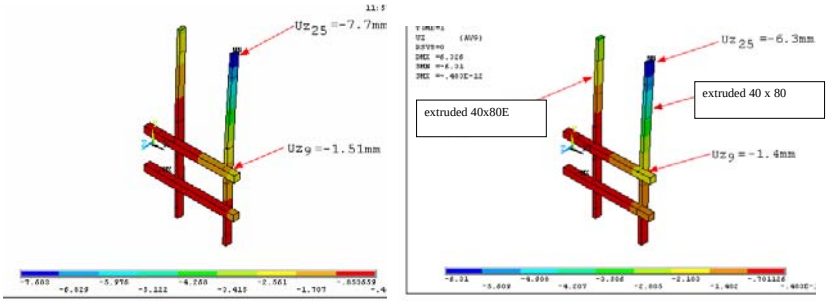

a) b)

Figure 10
Strain state of the optimized frame

Maximum deflection is 6.2 mm, which is rather high but localized at the end of one of the two 40x80 sections (node 25). Strain is fairly limited in the other areas of the frame. The maximum deflection could be reduced by replacing the most highly stressed component with one having better mechanical properties, such as a lightweight 40 x 80 section. This configuration would reduce maximum deflection to an acceptable 4.90 mm.
The optimization stage can thus be regarded as terminated.

Conclusions

Following the optimization stage, the frame will be constructed using two 80x80 E sections, two 40x80 E sections, and two lightweight 40x80 sections.
The data indicate that the mass of the structure drops from 58.62 kg to 43.04 kg, while maximum deflection increases from 3.77 to 4.90 mm. The reduction in mass is thus achieved at the cost of an increase in maximum deflection which is entirely acceptable from the standpoint of correct system operation. It is interesting to note that the most critical conditions occur when the frame is in configuration A.

Acknowledgements

The authors would like to thank Eng. D. Carle of Bottero S.p.A. (Cuneo, Italy) and Eng. A. Sciacovelli for their assistance.

References

[1] Taylor: Sensor robotics for handling of limp materials, 1990
[2] Dorf: International encyclopedia of robotics, 1988
[3] Chernousko: Manipulation robots, 1994
[4] Morgan: Robots, planning and implementation, IFS Publcations, 1984
[5] Kafrissen and Stephans: Industrial robots and robotics, Reston Publishing Company, 1984
[6] Carpinteri: Scienza delle costruzioni – 1, Pitagora Editrice (Bo, Italy), 1995